Empirical Characterization of Doppler in Industrial Wireless Channels

Dreyelian Morejón*, Jon Montalbán†, Eneko Iradier‡, Mohamed Kashef (Hany)§, Richard Candell§, Pablo Angueira*
*UPV/EHU: Dept. Communication Engineering, Bilbao, Spain, {dreyelian.morejon, pablo.angueira}@ehu.eus
†UPV/EHU: Dept. Electronics Technology, Bilbao, Spain, jon.montalban@ehu.eus
‡UPV/EHU: Dept. Computer Languages and Systems, Bilbao, Spain, eneko.iradier@ehu.eus
§NIST: National Institute of Standards and Technology, Gaithersburg, USA, {mohamed.kashef, rick.candell}@nist.gov

***Abstract*—This paper analyzes the temporal variation of the radio propagation channel in industrial environments. The results have been obtained by processing empirical data from the National Institute of Standards and Technology (NIST) in a field measurement campaign, at different industrial premises, with various dimensions and clutter densities. The paper analyzes the shape of the Doppler spectra and related parameters such as Doppler bandwidth and coherence time. The results are supplemented with maximum Delay Times and RMS Delay Spread data. The influence of factors such as the operational frequency band, environment, and polarization is also analyzed.**

***Index Terms*—Industrial communication, Wireless communication, Channel models, Doppler effect, Coherence time, Fading channels, Multipath channels.**

I. Introduction

The modernization of industrial production processes is one of the areas where wireless industrial communications can offer revolutionary benefits. Improvements in mobility, flexibility, scalability, deployment and maintenance costs, are classic advantages of wireless communications. Conversely, reliability, latency, and robustness against malicious attacks are challenges for these technologies. Several wireless communication standards and proprietary solutions are usable in industrial networks. However, they do not meet the specifications of every use case. This challenge is especially critical in the most demanding applications: Safety and Factory Automation. With this in mind, the IEEE 802.11 working group is currently developing a new version of the standard (IEEE 802.11bn Ultra High Reliability [1]), which is expected to solve an important part of the challenges of wireless communication in industrial applications in the coming years.

This paper contributes to the progress toward the general deployment of wireless systems in industry by analyzing, parameterizing, and validating the time-varying characteristics of the propagation channel. Determining these time-varying characteristics is crucial to success in standardization processes like those mentioned above. In addition, it is also fundamental for network deployment and planning methods and in the design of optimal algorithms in receivers.

There are two trends in channel modeling. On the one hand, 3GPP is working on geometric stochastic models derived from WINNER I/II [2], [3], which incorporate into their building blocks a considerable number of characteristics of the environment to which they are applied, at the cost of a significant complexity of adaptation. On the other hand, traditional channels of the Tapped Delay Line (TDL) type maintain their importance due to their versatility and ease of adjustment with a limited number of environmental and radioelectric data. This article contributes to the latter.

In summary, two contributions to the state of the art of Doppler modeling in industrial channels are proposed:

- Characterize the shape of the expected Doppler spectrum in different industrial environments.
- Obtain numerical values to describe the Doppler spectrum in industrial wireless channels.

The rest of the article is divided into the following sections. Section II presents previous work on the topic. Section III contains the description of the problem, its parameterization, the empirical data used, and their processing to obtain the reference variables used in the article. Section IV contains the results and their discussion. Finally, section V summarizes the conclusions of the paper.

II. Previous Works

Several measurement campaigns have been carried out in industrial environments, intended for more accurate characterization and modeling of the wireless channel. Research needs have been identified regarding the temporal characterization of the propagation channel in these environments. In [4], an analysis of the statistical and spatio-temporal characteristics of fading is presented. [5] presents an empirical study based on a measurement campaign in two wood processing and two metal processing factories, at 900, 2400, and 5200 MHz. The authors conclude that there is good agreement between the fading function and a Rician-type distribution in industrial environments. However, in [4], it was argued that this agreement is only possible in the presence of numerous moving scatterers, which is not applicable in most field measurements.

Trassl *et al.* [6] propose a Tapped Delay Line (TDL) channel model that includes all the functions that usually make up these models. In his model, Trassl questions using Jake's Doppler model because, although its use is widespread, it is

only sometimes justified. Trassl proposes the Laplacian model as an alternative. A small dispersion of the angles of arrival characterizes this model.

In the area of empirical channel measurement databases, several open-access sources are available. On the one hand, the measurements of the National Institute of Standards and Technology (NIST) of the USA [7] stand out for their timeliness and accuracy. Another source is the Community Resource for Archiving Wireless Data At Dartmouth (CRAWDAD) repository [8]. In the case of industrial communications, the *init/factory* dataset includes several measurements with some limitations, i.e., the database size and the type of motion (static receiver and people moving around it).

Finally, and in line with the data processing of this paper, in [9], a methodology for segmenting measurements in time is presented to better identify the different propagation conditions that may be present in a given environment.

III. Methodology

This section describes the parameters involved in Doppler characterization, the empirical data used, and the processing designed to obtain numerical reference values.

A. Problem Description and Parametrization

In the general channel model outlined in Fig. 1, each block accounts for different physical phenomena involved in the propagation process. This article contributes to the modeling of the *Temporal Correlation* block. Additionally, it also provides valuable information for the *Fading Statistics* module.

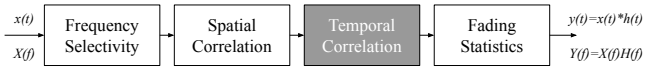

Fig. 1: Block diagram of the channel model.

First, selecting the function that describes the Doppler spectrum is not straightforward. One of the most commonly used models for Doppler spectrum is Jake's model, which assumes that all rays arrive with equiprobable Angles of Arrival (AoA). Trassl *et al.* question using Jake's spectrum, and propose using a Laplacian distribution. The Laplacian Doppler spectrum is modeled by two parameters: the arrival angle and the angular dispersion. A Laplacian Doppler with a high angular dispersion would result in a Jake's Doppler. Finally, the *Fading Statistics* module accounts for amplitude fading statistics. Rice or Rayleigh fading is assumed and described by the corresponding fading statistics model. Among the parameters that can be used to characterize the Doppler spread and multipath, we have analyzed the ones listed in Table I.

B. Empirical Data

The empirical data used in this work correspond to experimental measurements carried out by NIST [7]. This data comprises a large repository of propagation measurements conducted in three different industrial facilities: an automotive factory (AF), a steam generation plant (SGP), and a mechanical workshop (MW) [7].

TABLE I: Analyzed Doppler-related parameters.

Parameter	**Physical Meaning**
Doppler Spectrum Shape	Scattering and Angular distributions
Doppler Spread [Hz]	Motion caused Max Spectrum Widening
Coherence Time [ms]	Interval where channel is quasi-invariant
RMS Delay Spread [ns]	Multipath richness of a channel
Mean Delay [ns]	Observed Energy Time Dispersion

The channel sounder employed for measurements is a Pseudo Noise sequence correlation-based system. The transmit antenna used was either an omnidirectional or a horn antenna. The receive antenna used for all measurements was an omnidirectional dipole [10].

Measurements were performed under normal operating conditions, at 2.245 GHz and 5.4 GHz, with a moving receiver following specific routes and testing different receiver antenna polarizations. All routes are highly obstructive, predominantly non-line-of-sight (NLOS), with K-factor values ranging from -5 dB to 6 dB [10]. Table II summarizes the datasets.

TABLE II: Empirical Source data from NIST.

Environment	**Dimensions**	**Route**	**Datasets**
Automotive factory (AF)	Area: 400x400 m2 Height: 12 m	Outer: 870m Inner: 400m	Outer: 8 Inner: 8
Steam generation plant (SGP)	Area: 20x80 m2 Height: 7.6 m	140m	15
Mechanical workshop (MW)	Area: 12x15 m2 Height: 7.6 m	315m	18

The measurements include raw IQ data from both, moving and static situations. These recordings were processed to obtain the instantaneous channel impulse responses (CIR) at each location, with a set of associated metadata [10].

C. Data Processing

The Doppler bandwidth has been obtained from the calculation of the Scattering Function for each time instant by using the sliding window method. The Scattering Function represents the expected power of the received signal as a function of the Doppler shift ν and the excess delay τ. It is related to the delay-time CIR ($h_{\tau,t}$) by the following analytical relationship [11], where $FT\{\cdot\}$ represents the Fourier Transform:

$$S_{\tau,\nu} = \left|FT\left\{h_{\tau,t}\right\}\right|^2. \tag{1}$$

The width of the window used to calculate $S_{(\tau,\nu)}$ at every time instant, is set to the period where the channel shows a quasi-stationary behavior, ensuring that the filtering does not eliminate essential characteristics of the channel. According to the results in [12], the sliding window should be extended between 10 and 40 wavelengths (λ). After extensive testing, a 40λ window was chosen. Assuming that the receiver is moving

at an average speed of v = 1.4 m/s (i.e., pedestrian speed), the number of samples for a 40λ window is an inverse function of the period between the CIRs (T_S), and is calculated as follows:

$$N_W = \frac{40\lambda}{v \cdot T_S}. \quad (2)$$

The window widths used in the investigated datasets vary between 77 and 207 samples. These values satisfy Lee's minimum criteria and guarantee a sufficient number of samples to obtain a reliable frequency spectrum. The Doppler spectrum corresponding to each window is obtained from $S_{(\tau,\nu)}$ using the following relationship, where N_τ is the total number of multipath elements:

$$S_\nu[k] = \sum_{n=0}^{N_\tau - 1} S_{\tau,\nu}[n,k]. \quad (3)$$

Doppler bandwidths (BW_D) reported in this paper are over frequencies associated with 99% of the spectral energy of S_ν.

The channel coherence times (T_C) values obtained from the autocorrelation function are also considered. To obtain the autocorrelation function, the inverse fast Fourier transform (IFFT) of every S_ν obtained by the sliding window method is calculated. The values of T_C for every time instant are obtained by measuring the interval where the central lobe of the autocorrelation function is above 50% of its maximum.

IV. Results and Discussion

A. Global Results

Table III summarizes all the metrics obtained from the dataset processing. The corresponding metrics were previously calculated for each time point of each individual measurement run (i.e., for each dataset). The values shown in Table III, which correspond to the averages of the median values of each of these metric distributions, are grouped according to environment and frequency criteria. Considering the fact that we are analyzing results with many outliers that can induce false trends in the metrics, the median of each metric is used because it is a statistical measure that focuses on the mean data of the set and gives little importance to the extreme values.

TABLE III: Parameter values from empirical data.

Site	Freq. [GHz]	BW_D [Hz]	T_C [ms]	$\bar{\tau}$ [ns]	τ_{RMS} [ns]
Automotive fact. inner route (AFin)	2.245	29.32	69.35	606.27	106.23
	5.4	40.01	34.2	726.78	177.36
Automotive fact. outer route (AFout)	2.245	21.15	104.33	457.49	130.3
	5.4	35.52	54.63	508.46	153.8
Steam generation plant (SGP)	2.245	18.51	207.33	88.57	35.36
	5.4	36.26	61.59	123.54	44.74
Mechanical Workshop (MW)	2.245	22.56	82.95	146.76	62.75
	5.4	40.49	43.2	122.92	57.19

NIST datasets include data of measurements obtained in co-polarization (i.e. both transmitter and receiver antennas in vertical polarization) and in cross-polarization (i.e. transmitter antenna in vertical polarization and receiver in horizontal polarization) conditions. We analyze the influence of cross-polarization in every metric discussed in this work. However, unless explicitly stated, the results are presented for co-polarization conditions.

B. Doppler spectrum shape

The selection of a mathematical model to characterize Doppler scattering in industry involves the analysis of its spectral structure in actual industrial environments. In a previous work [11], we obtained the Doppler spectrum for a subset of NIST data and observed a significant influence of receiver mobility in the spectral distributions. The datasets show that the only file that contains static segments is the one corresponding to the inner route of the AF facility (AFin), in which approximately two minutes of static measurements were taken in each run.

In Fig. 2 is shown the aggregated Doppler spectral distributions for all environments. To better analyze the mobility effect on the Doppler spectrum, we have separated the measurements corresponding to all the static segments at AFin.

Figs. 2a and 2b show the critical influence of receiver motion on the shape of the Doppler spectral distribution. The spectrum corresponding to the moving receiver shows a dispersion whose width seems to be influenced by the receiver's speed and link frequency. On the other hand, the spectrum corresponding to the aggregation of the static sections is independent of frequency and concentrates towards the center, with a shape similar to a Laplacian function. Also note that, although sharply concentrated around the center, the static spectrum for 2.245 GHz is slightly broader than the one at 5.4 GHz. This could be indicative of a higher influence of the environment at lower frequencies.

As observed in Figs. 2b to 2e, it only approximates Jake's spectrum in the bigger environments (AF inner and outer routes), whose more dense multipath condition approaches better Jake's assumption of uniformly distributed AoAs. Spectrum shapes are closer to Rectangular or Gaussian distributions for the smaller environments (MW and SGP).

The spectra at the right side in Fig. 2 correspond to measurements with cross-polarization conditions. The NIST datasets do not contain cross-polarization measurements for the SGP at 2.245 GHz, so these spectra are missing from Fig. 2e. A decrease in signal level compared to the co-polarization condition is observed in all cases. For the distributions associated with a moving receiver in cross-polarization conditions, the U-shape characteristic of Jake's model almost fades out in all cases, getting closer to Gaussian-like distributions. In the case of the distributions corresponding to a static receiver, the Laplacian-shaped spectrum remains almost the same.

C. Doppler spread

Fig. 3 presents boxplot formatted Doppler bandwidth distributions for all mobility conditions (i.e. static and moving). The values have been normalized to the sampling frequency

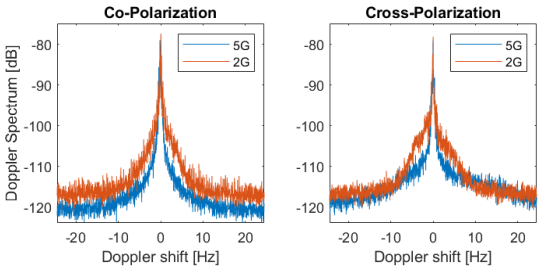

(a) Static segments at inner route of automotive factory

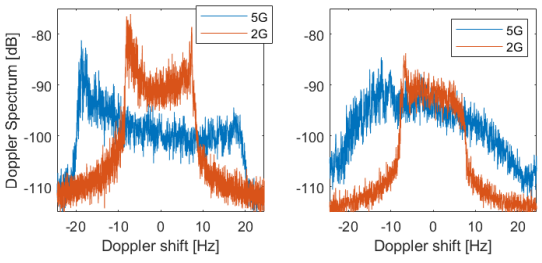

(b) Moving segments at inner route of automotive factory

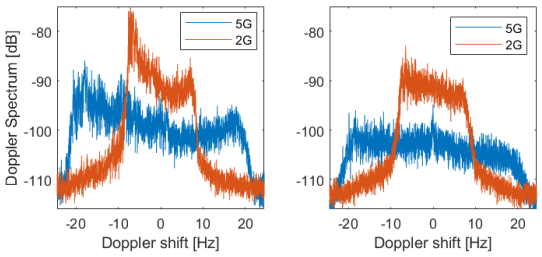

(c) Outer route of automotive factory

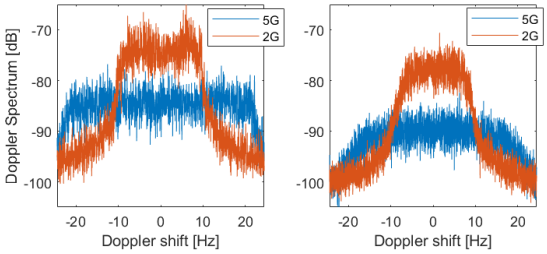

(d) Mechanical workshop

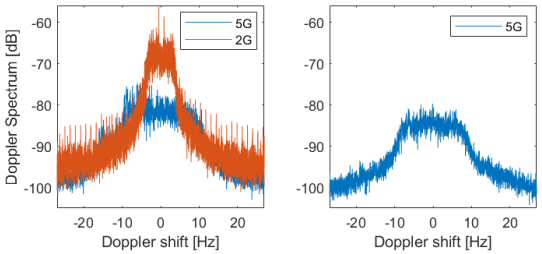

(e) Steam generation plant

Fig. 2: Aggregated Doppler spectrums segmented by mobility and antenna polarization for every environment.

(sounding frequency), as a common reference to compare all datasets.

The results show a direct proportionality between Doppler spreads and frequency, which is consistent with the expected

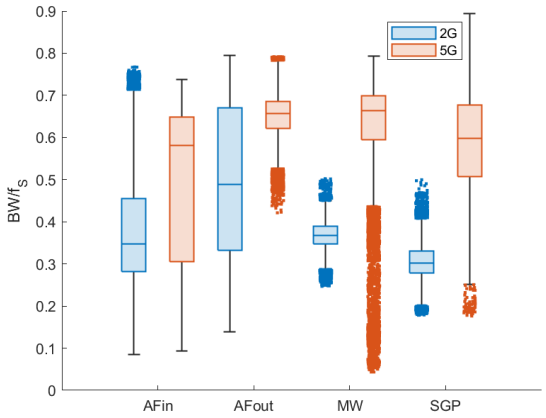

Fig. 3: Doppler spread for every site.

behavior of this parameter.Note also that, in contrast to what happens at 5.4 GHz, there is a tendency for the Doppler spread dispersion to decrease for smaller environments at the 2.245 GHz frequency. This behavior could be explained by considering that the Doppler spreads are determined by two fundamental factors: the receiver's mobility and the surrounding elements' mobility. The higher the multipath, the greater the influence of the surrounding elements, which strongly depends on the number of rays reflected by them. In smaller rooms with less time dispersion, the Doppler spread should be concentrated mainly around the deviations caused by the average speed of the receiver. In the case of the 5.4 GHz behavior, although the multipath is higher at this frequency, the attenuation also increases significantly, accentuating the difference between the levels of the clusters reflected by the surrounding elements, compensating each other, so that there is no clear trend in this case.

D. Coherence time

Fig. 4 shows boxplot graphics of the coherence time distributions as a function of the environment and frequency. As in the case of the Doppler spreads, the values have been normalized to the sampling interval.

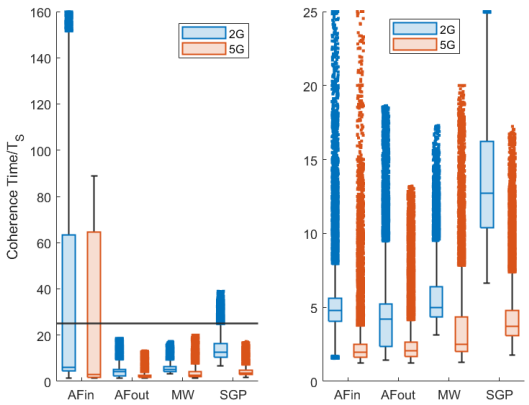

Fig. 4: Coherence time at every site for both static and moving segments (left) and only for moving segments (right).

The values obtained along the inner route of the Automotive Plant (AFin) on the left plot (including both static and moving segments) stand out. Although the median values are at a similar level to the other routes, the relative dispersion of the values is remarkable, with coherence times exceeding 60 sampling intervals. This behavior can be explained by considering that in this run the receiver was kept static for intervals of more than two minutes. To isolate the influence of the mobility, the metrics corresponding to this run were separated into static and moving segments, according to the mobility of the receiver. As a result, the coherence time values obtained for the mobile segments of the inner path were similar to those obtained for the outer path (Fig. 4 right). In the case of Doppler spreads, the mobility effect is mainly reflected in a higher spread toward lower values of BW_D at 5.4 GHz, but is almost unnoticeable at 2.245 GHz. The high relative values of T_C obtained for the static segment give a measure of the negative impact of the Doppler effect in a wireless link. It should be noted how mobility affects the coherence times much more than the Doppler spread. This fact also gives a measure of the large variability of the uncertainty relation $BW_D \cdot T_C$ as a function of environment and mobility.

Among the other measurement routes, the one corresponding to the SGP at 2.245 GHz frequency stands out. In this sense, it should be noted that this environment is one of the most obstructive of all those analyzed. This is confirmed by the observation in Table III that the average propagation time at 2.245 GHz for this environment is almost half that of the other environments of similar dimensions, even when compared with itself at 5.4 GHz. Therefore, in this case, since the arrival of reflections is limited, the influence of moving elements in the environment is also less prominent.

As part of this work, we investigated the influence of link polarization on coherence times or Doppler spreads, but no significant correlation was found.

V. Conclusion

Modeling and analysis of temporal fading is a relevant issue in the industry scenario. NIST measurement datasets comprise a large repository of wireless propagation measurements carried out on a representative set of industrial environments for 2.4 and 5.4 GHz frequencies, under several measurement conditions and a convenient temporal resolution in the order of milliseconds. Using the sliding window method and proper analytical processing of the raw data, those datasets have been used to calculate Doppler spectrums, Doppler spreads and coherence times for each time instant.

A determinant influence of receiver motion was observed for all parameters analyzed. The spectrum corresponding to static sections is independent of frequency and resembles a centered Laplacian function. For moving receiver sections, the spectrum distribution shows more variability in width and shape, depending on receiver speed, link frequency, and physical environment.

For Doppler spreads, the results have verified its functional direct relationship with frequency. It has been found for the measurements at 2.245 GHz, a trend to reduction in Doppler spread dispersion for smaller-sized environments.

Static segments were found to increase significantly the coherence times. In general, mobility affects the coherence times more strongly than they do with Doppler spreads, so giving a measure of the large variability of the uncertainty relation $BW_D \cdot T_C$ as a function of the environment and mobility. Finally, no significant influence of antenna polarization was found, neither in coherence times nor in Doppler spreads.

Work is currently continuing on future field tests in industrial environments that can complement and extend the results of this work.

Disclaimer

Certain commercial equipment, instruments, or materials are identified in this paper in order to specify the experimental procedure adequately. Such identification is not intended to imply recommendation or endorsement by the National Institute of Standards and Technology, nor is it intended to imply that the materials or equipment identified are necessarily the best available for the purpose.

References

[1] E. Reshef and C. Cordeiro, "Future directions for WI-FI 8 and beyond," vol. 60, no. 10, pp. 50–55, 2022.

[2] J. Bian, J. Sun, C.-X. Wang, R. Feng, J. Huang, Y. Yang, and M. Zhang, "A winner+ based 3-d non-stationary wideband mimo channel model," *IEEE Transactions on Wireless Communications*, vol. 17, no. 3, pp. 1755–1767, 2018.

[3] K. Haneda, L. Tian *et al.*, "Indoor 5g 3gpp-like channel models for office and shopping mall environments," in *2016 IEEE International Conference on Communications Workshops (ICC)*, 2016, pp. 694–699.

[4] Q. Zhang, Q. Zhang, W. Zhang, F. Shen, T. H. Loh, and F. Qin, "Understanding the temporal fading in wireless industrial networks: Measurements and analyses," in *2018 10th International Conference on Wireless Communications and Signal Processing (WCSP)*, 2018, pp. 1–6.

[5] E. Tanghe, W. Joseph, L. Verloock, L. Martens, H. Capoen, K. V. Herwegen, and W. Vantomme, "The industrial indoor channel: large-scale and temporal fading at 900, 2400, and 5200 mhz," *IEEE Transactions on Wireless Communications*, vol. 7, no. 7, pp. 2740–2751, 2008.

[6] A. Traßl, T. Hößler, L. Scheuvens, N. Franchi, and G. P. Fettweis, "Deriving an empirical channel model for wireless industrial indoor communications," in *2019 IEEE 30th Annual International Symposium on Personal, Indoor and Mobile Radio Communications (PIMRC)*, 2019, pp. 1–7.

[7] R. Candell, "Radio frequency measurements for selected manufacturing and industrial environments." [Online]. Available: http://doi.org/10.18434/T44S3N

[8] D. Kotz and T. Henderson, "CRAWDAD: A community resource for archiving wireless data at dartmouth," vol. 4, no. 4, pp. 12–14, 2019.

[9] M. Kashef, R. Candell, and Y. Liu, "Clustering and representation of time-varying industrial wireless channel measurements," in *IECON 2019 - 45th Annual Conference of the IEEE Industrial Electronics Society*, vol. 1, 2019, pp. 2823–2829.

[10] R. Candell, K. A. Remley, J. T. Quimby, D. Novotny, A. Curtin, P. B. Papazian, M. Kashef, and J. Diener, "Industrial wireless systems radio propagation measurements," p. NIST TN 1951. [Online]. Available: https://doi.org/10.6028/NIST.TN.1951

[11] D. Morejón, E. Iradier, P. Angueira, and J. Montalban, "Empirical delay and doppler profiles for industrial wireless channel models," in *2023 IEEE 19th International Conference on Factory Communication Systems (WFCS)*, 2023, pp. 1–4.

[12] W. Lee, "Estimate of local average power of a mobile radio signal," *IEEE Transactions on Vehicular Technology*, vol. 34, no. 1, pp. 22–27, 1985.